[1]Adesh K. Mishra*
[2] S. M. Tripathi
[3] Omveer Singh

Real-time Assessment of Ride-through Capability of Grid-tied Converter in Renewable Power Applications

Journal of Electrical Systems

Abstract: This paper presents a comprehensive strategy for controlling grid-tied converters, with the primary goal of seamlessly integrating renewable power sources into the grid while ensuring stability and reliability. The control strategy is designed to achieve unity power factor operation under normal grid conditions, while also adhering to ride-through requirements to withstand voltage dips. Using the Typhoon HIL604 real-time simulation platform, extensive testing of the grid-tied converter is conducted to validate its performance. The results of the performance assessment are thoroughly analyzed and presented to exemplify the efficacy of the proposed control strategy. Notably, the paper emphasizes the converter's operation at unity power factor during normal grid conditions, indicating maximized active power delivery to the grid. Furthermore, the grid-tied converter demonstrates impressive ride-through capability during symmetrical voltage dip, achieved through the dynamic adjustment of grid current references to maintain grid stability. This research contributes to the advancement of grid-tied converter control strategies, offering insights into enhancing the integration of renewable power sources into the power grid while upholding system reliability and stability. Overall, this research offers valuable insights into the practical implementation of grid-tied converters for renewable power integration. It presents a comprehensive control strategy that not only enhances the integration of renewable power sources into the power grid but also prioritizes system reliability and stability.

Keywords: Grid-tied converter, real-time simulation, ride-through capability, Typhoon HIL simulator, unity power factor operation, voltage dip.

I. INTRODUCTION

In recent years, the global effort to address climate change and transition towards sustainable energy systems has accelerated, driving a remarkable surge in the integration of renewable power sources into power grids [1]. This shift reflects a growing recognition of the urgent need to diminish greenhouse gas emissions and reliance on fossil fuels in the energy sector. However, the transition to renewable energy presents unique challenges due to the inherently irregular nature of renewable power sources [2, 3]. Unlike traditional fossil fuel-based power generation, renewable power sources exhibit variability in their generation patterns, influenced by factors such as weather conditions, time of day, and seasonal changes. These fluctuations can lead to mismatches between power generation and demand, posing significant implications for grid stability and reliability [2].

The irregular nature of renewable power sources underscores the critical importance of advancing grid-tied converter technologies [3]. Grid-tied converters play a vital role in facilitating the integration of renewable power sources into existing power infrastructure by converting the variable output of renewable power sources into stable and synchronous electricity that can be seamlessly integrated into the grid [4–6]. Through sophisticated control algorithms and innovative hardware designs, grid-tied converters enable efficient energy conversion and grid synchronization, ensuring optimal utilization of renewable power sources while ensuring grid stability and reliability. As the global energy landscape continues to evolve, the role of grid-tied converters in enabling the seamless integration of renewable power sources becomes increasingly vital. By addressing the challenges posed by the variability of renewable power generation, these converters contribute to the ongoing transition towards a more sustainable and resilient energy system. Continued research and development efforts in grid-tied converter technologies are essential to unlocking the full potential of renewable power and accelerating the transition towards a low-carbon future.

The control strategy adopted for grid-tied converters focuses on several key objectives: ensuring synchronization with the grid, maintaining power quality, providing reactive power support to the grid, and regulating DC link capacitor voltage [3, 7, 8]. Additionally, maintaining unity power factor operation in grid-tied converters is indispensable for maximizing active power delivery to the grid [5–7]. This is critical for efficient energy utilization, grid stability, and seamless integration of renewable power sources into the grid. Extensive research has been conducted to explore various control designs for grid-tied converters, with some of these control designs briefly reviewed in existing literature [3, 7–18]. The development of advanced grid-tied converter technologies and control strategies is crucial for addressing the challenges posed by the integration of renewable

[1] *Corresponding author: Electrical Engineering Department, Gautam Buddh University, Greater Noida–201312, India; adesh143mishra@gmail.com
[2] Power & Energy Research Centre, Electrical Engineering Department, Kamla Nehru Institute of Technology, Sultanpur–228118, India; mani@knit.ac.in
[3] Electrical Engineering Department, Gautam Buddh University, Greater Noida–201312, India; omveer.singh@gbu.ac.in

power sources into power grids, ultimately contributing to the transition towards a more sustainable and resilient energy infrastructure.

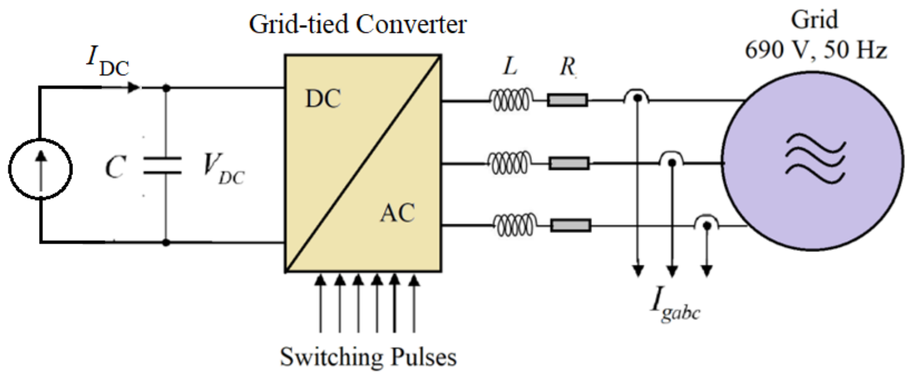

Fig.1. Schematic of a grid-tied converter.

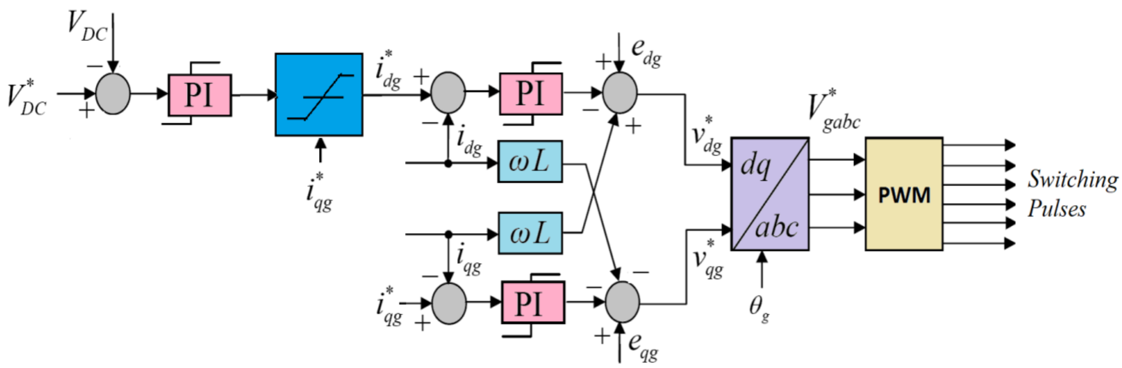

Fig.2. Proposed strategy for grid-tied converter control and operation.

The ride-through capability of grid-tied converters plays a pivotal role in ensuring the seamless and uninterrupted operation of renewable power generation systems, particularly during adverse grid conditions such as grid voltage dips [8, 11]. By effectively riding through grid disturbances, these converters help maintain grid stability, minimize power disruptions, and enhance the overall reliability of renewable power generation [11, 19–21].

In essence, dedicated grid codes issued for grid-tied converters impose stringent requirements for ride-through compliance, mandating these converters to remain interconnected with the grid even in the face of short-duration voltage dips [8, 11, 18, 20]. This regulatory framework underscores the importance of ensuring that grid-tied converters possess robust ride-through capabilities to meet the stringent grid code requirements and maintain grid stability during transient grid events.

The ability of grid-tied converters to effectively ride-through grid disturbances not only enhances the reliability of renewable power generation but also contributes to the overall resilience of the power grid. It enables renewable power generation systems to continue supplying power to the grid even during abnormal grid conditions. Therefore, the ongoing development and enhancement of ride-through capabilities in grid-tied converters remain imperative for the continued growth and integration of renewable power sources into the power grid.

Testing the ride-through capability of grid-tied converter control using real-time simulators is indispensable for validating its performance under grid voltage dip conditions. This testing not only ensures the reliability and robustness of the designed control algorithm but also guarantees the effectiveness of the grid-tied converter in maintaining grid stability amidst dynamic grid conditions. Consequently, the real-time assessment of ride-through capability emerges as a critical aspect in the design, deployment, and operation of grid-tied converters for renewable power applications.

A control strategy devised for grid-tied converters is explored here, primarily focusing on achieving unity power factor operation under normal grid conditions. The proposed strategy aims to enhance transient response, ensure reliable performance during steady-state operation, and minimize power ripples through internal current control loops. Additionally, the paper conducts a comprehensive investigation into the real-time assessment of ride-through capability in grid-tied converter utilized in renewable power applications. To assess the performance of the grid-tied converter, a real-time simulation test bench is established, employing the Typhoon HIL 604 platform. Through real-time experimental validations, this paper aims to provide valuable insights into the performance and effectiveness of ride-through techniques under symmetrical voltage dip condition.

The remaining part of the paper is structured as follows: Section II provides an overview of the grid-tied converter. Section III discusses the control strategy aimed at enhancing its ride-through capability. Section IV presents real-time assessments of the performance and ride-through capability of the grid-tied converter. Finally, Section V sums up the main findings and suggests ideas for future research.

II. Grid-tied Converter

The diagram in Fig.1 illustrates the schematic of a grid-tied converter, a crucial element in transferring active power generated by renewable sources to the grid. Within this schematic, the current source symbolizes the equivalent DC current output from the renewable power source. This DC current is then supplied to the grid-tied inverter, where it undergoes conversion into AC with voltage and frequency levels compatible with the utility grid. Serving as an intermediary, the grid-tied converter ensures the smooth integration of renewable power sources into the existing grid infrastructure. The grid voltage equations are represented [8, 11, 22, 23] as follows (1) and (2), where e_{dg} and e_{qg} are the grid voltages along the *d*-axis and *q*-axis respectively, R denotes the coupling resistance, L stands for coupling inductance, v_{dg} and v_{qg} are the *d*-axis and *q*-axis converter voltages, and ω signifies the angular frequency of the grid.

$$e_{dg} = Ri_{dg} + L\frac{di_{dg}}{dt} - \omega L i_{qg} + v_{dg} \tag{1}$$

$$e_{qg} = Ri_{qg} + L\frac{di_{qg}}{dt} + \omega L i_{dg} + v_{qg} \tag{2}$$

III. Control Description

The voltage-oriented control is utilized to control the grid-tied converter [4, 6–8, 11], as depicted in Fig. 2. In this scheme, a proportional-integral (PI) controller for the DC-link voltage compares the reference and actual values of the DC-link voltages. It then adjusts any voltage deviations to derive the *d*-axis reference grid current i^*_{dg} according to the following equation:

$$i^*_{dg} = K_{pv}\left(\frac{1+pT_{iv}}{pT_{iv}}\right)\cdot(V^*_{DC} - V_{DC}) \tag{3}$$

where K_{pv} and T_{iv} denote the proportional gain and the integral time constant, respectively, of the PI controller for the DC-link voltage.

Conversely, to maintain a power factor of unity for the grid-tied converter operation, the reference value of the grid current along the *q*-axis i^*_{qs} is put to zero [4, 7]. In the event of a grid-voltage dip, adherence to the ride-through requirement is ensured by appropriately adjusting the *q*-axis reference grid current in accordance with the E.ON Netz fault-response code [24]. Consequently,

$$i^*_{qg} = \begin{cases} 0 & ; \quad 0.9E_g \le E_{g\_dip\_condition} \\ 2\times\dfrac{(E_g - E_{g\_dip\_condition})}{E_g}\times I_{g\max} & ; \quad 0.5E_g < E_{g\_dip\_condition} < 0.9E_g \\ I_{g\max} & ; \quad 0.5E_g \ge E_{g\_dip\_condition} \end{cases} \tag{4}$$

where E_g is the grid voltage in normal grid condition and is given by:

$$E_g = (e^2_{dg} + e^2_{qg})^{\frac{1}{2}} \tag{5}$$

and $E_{g\_dip\_condition}$ is the grid voltage during dip condition.

Meanwhile, the *d*-axis reference grid current i^*_{dg} is constrained as follows:

$$\left| i^*_{dg} \right| \leq (I^2_{g\max} - i^{*2}_{qg})^{\frac{1}{2}} \tag{6}$$

In current control loops, PI controllers analyze the actual *d*-*q* axes grid currents i_{dg} and i_{qg} in comparison to their reference values, making necessary adjustments to rectify any deviations. As a result, reference values are established for both the *d*-axis and *q*-axis converter voltages v^*_{dg} and v^*_{qg}. These voltages are then inversely transformed to derive the three-phase reference converter voltages V^*_{gabc}. These values are subsequently utilized by the pulse width modulator (PWM) to generate switching signals for the grid-tied converter.

This study also addresses the enhancement of the ride-through capability of grid-tied converters. It focuses on constraining the DC current input to the converter during grid voltage dips to ensure that the DC-link voltage remains within acceptable limits. Consequently,

$$I_{DC} = \begin{cases} \dfrac{P_{DC}}{V_{DC}} & ; \quad \text{Normal Condition} \\ \dfrac{\kappa\, P_g}{V_{DC}} & ; \quad \text{Voltage Dip Condition} \end{cases} \tag{7}$$

where P_{DC} stands for the equivalent DC power produced by the renewable power source, while P_g indicates the active power transferred to the grid, and $\kappa = 0.9$.

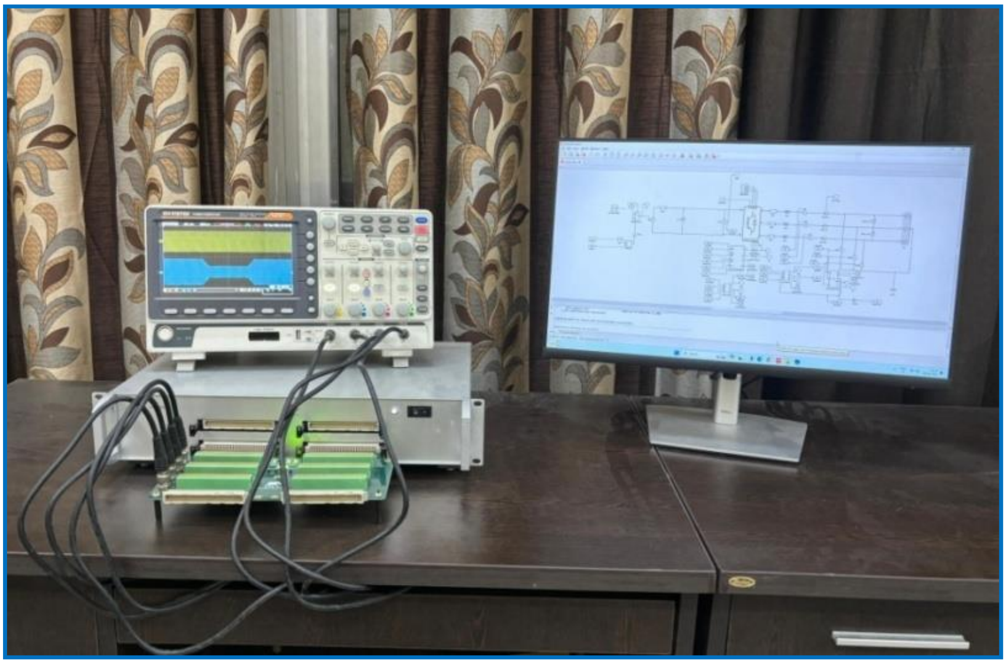

Fig. 3. Real-time simulation test setup with Typhoon HIL 604 emulator.

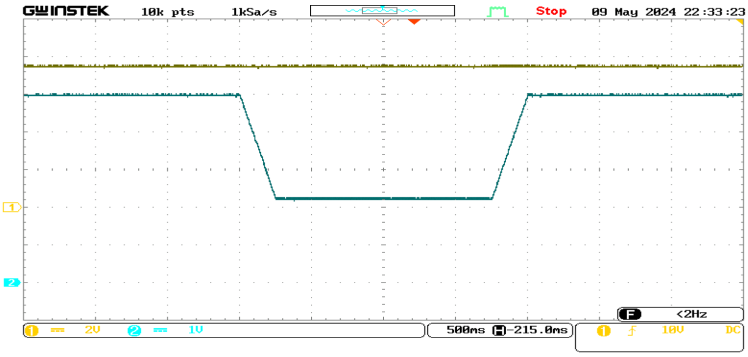

(a)

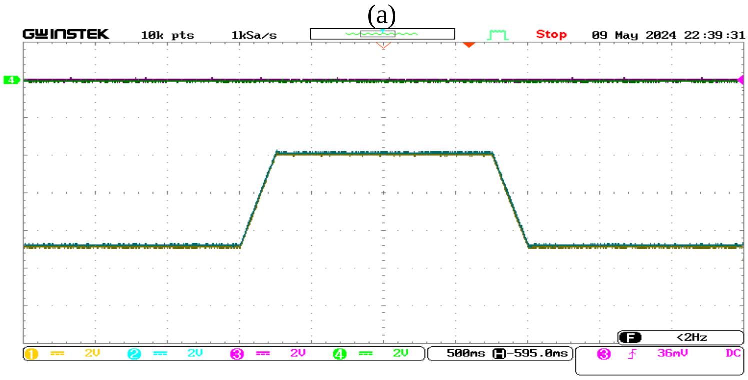

(b)

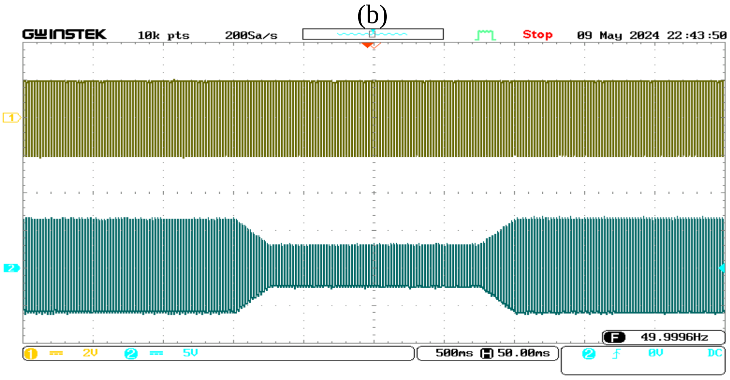

(c)

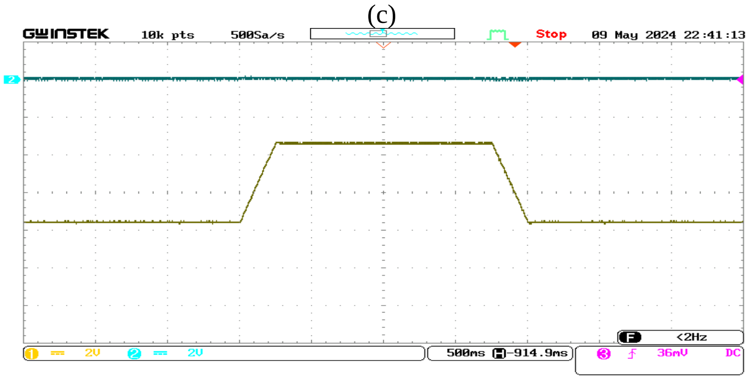

(d)

Fig. 4. The response of the grid-tied converter to gradual changes in DC current input under normal grid conditions, ranging from 995 A to 445 A and back to 995 A within a short duration—(a) CH-1: DC link capacitor voltage (400 V /div), CH-2: DC current input (200 A /div); (b) CH-1 and CH-2: actual and reference *d*-axis grid currents, respectively (400 A /div), CH-3 and CH-4: actual and reference *q*-axis grid currents, respectively (400 A /div); (c) CH-1: grid voltage (400 V /div), CH-2: grid current (1000 A /div); (d) CH-1: active power supplied to the grid (400 kW /div), CH-2: reactive power transfer between grid-tied converter and the grid (400 kVAR /div).

IV. Real-time Simulation Results

To showcase the dynamic performance of the grid-tied converter under both normal grid conditions and during ride-through compliance amid grid voltage dips, a real-time simulation model is developed and tested using the Typhoon HIL604 emulator, as illustrated in Fig. 3. The system parameters are provided in Appendix. Figs. 4–5 provide a detailed insight into the performance of the grid-tied converter through various test results. These results are crucial for understanding how the converter behaves under different operational conditions. Specifically, the tests demonstrate the grid-tied converter's response to gradual changes in input DC current, which varies from 995A to 445A and back to 995A within a short duration. This dynamic scenario highlights the adaptability and effectiveness of the control strategy employed.

In Fig. 4(a), the control strategy effectively maintains the DC link capacitor voltage at a constant level amidst changes in input DC current. This consistency is vital for ensuring stable operation and aligning the capacitor voltage with the reference value of DC-link capacitor voltage, demonstrating the efficacy of the control strategy. As depicted in Fig. 4(b), while the *d*-axis grid current adapts to changes in DC input current, the *q*-axis grid current remains consistently at zero. This behavior underscores the ability of the control strategy to track the *d*-*q* axes grid currents to respective reference values with minimal deviation.

Fig. 4(c) illustrates noticeable changes in the magnitude of grid current despite the constant magnitude of the grid voltage, attributed to variations in the input DC current. This demonstrates the adaptability of the grid-tied converter in maintaining reliable performance by adjusting accordingly. Additionally, Fig. 4(d) showcases the gradual changes in active power transferred to the grid in correlation with variations in the input DC current, while the reactive power remains closer to zero. Additionally, as illustrated in Fig. 5, both the grid voltage and current display sinusoidal patterns, confirming that the grid-tied converter operates with a unity power factor and efficiently transfers active power to the grid.

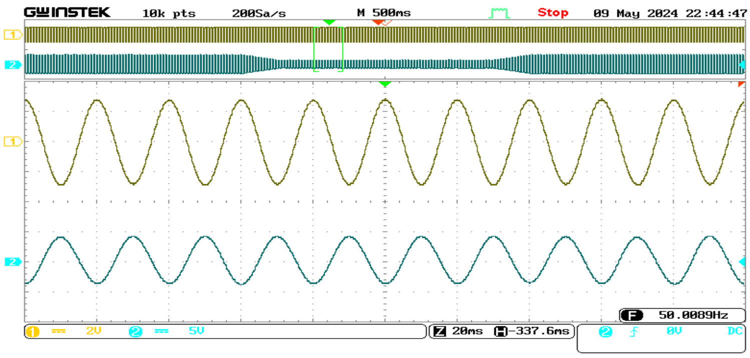

Fig. 5. Zoomed view of grid voltage and grid current under normal grid condition—CH-1: grid voltage (400 V /div), CH-2: grid current (1000 A /div).

In addition to the analysis under normal grid conditions, this paper also investigates the performance of the grid-tied converter under adverse grid condition; particularly during a 50% symmetrical voltage dip lasting 200 ms, as depicted in Fig. 6. This assessment aims to evaluate the converter's ability to withstand and recover from transient grid voltage dip, thus assessing its ride-through capability. During the real-time simulation, the input DC current is initially set at 995 A, and the results are presented in Fig. 6. It is noticed that during the symmetrical grid-voltage dip, the average *q*-axis grid currents reach approximately 1775 A, as shown in Fig. 6(b). This indicates the provision of reactive current support to the grid, alongside a limited transfer of active power (see Fig. 6(d)).

While ensuring ride-through compliance during symmetrical grid-voltage dip condition, there arises an excess of active power due to the disparity between the power produced by the renewable source and the active power supplied to the grid. This surplus power can lead to a raise in the DC link capacitor voltage. However, the implementation of specific control measures is effective in mitigating this issue, as evidenced by Fig. 6(a), where the DC-link voltage remains within acceptable limits. This strategic control helps enhance the ride-through capability of the grid-tied converter by ensuring stable operation during transient grid voltage dip.

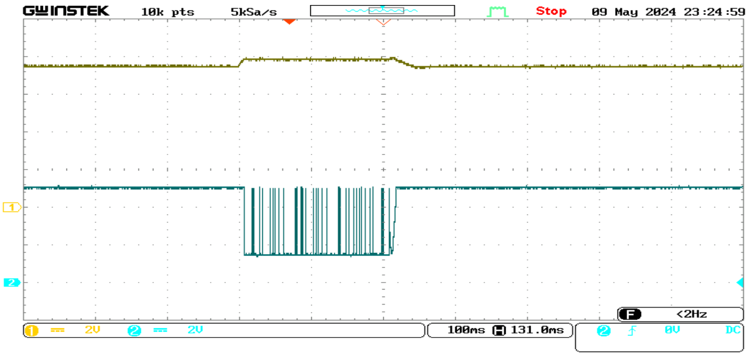

(a)

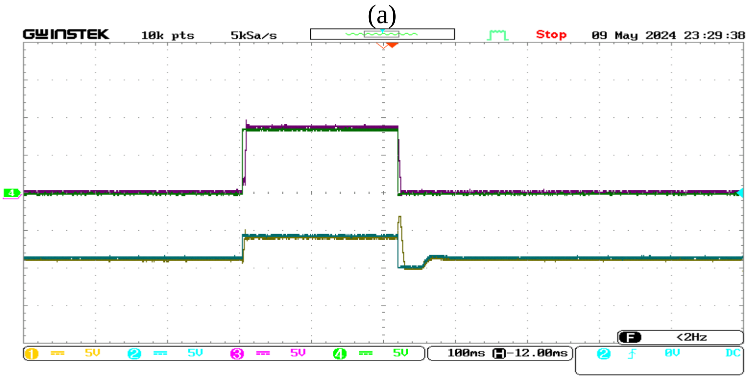

(b)

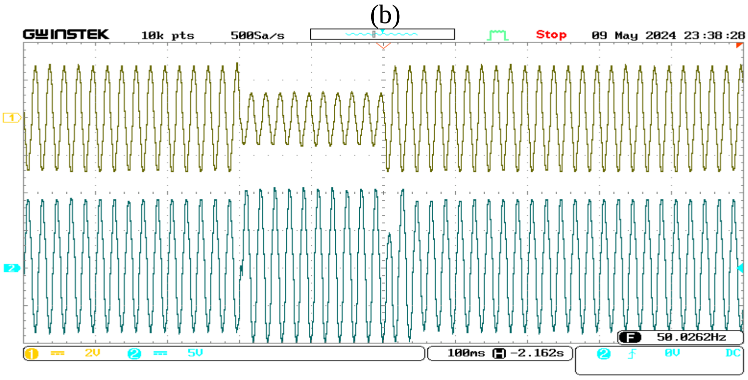

(c)

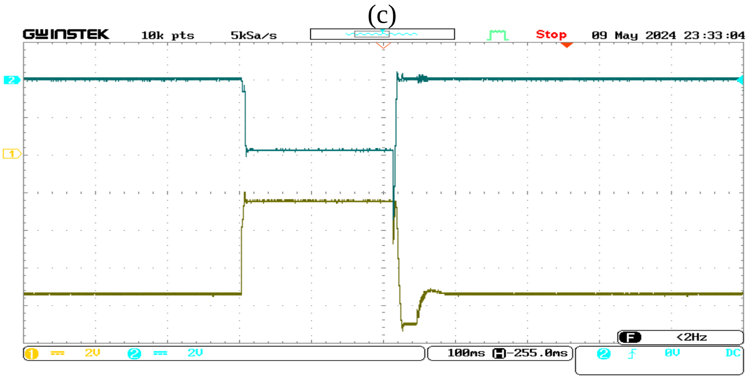

(d)

Fig. 6. Demonstration of the ride-through capability of the grid-tied converter during a symmetrical grid voltage dip condition lasting 200 ms—(a) CH-1: DC link capacitor voltage (400 V /div), CH-2: DC current input (400 A /div); (b) CH-1 and CH-2: actual and reference *d*-axis grid currents, respectively (1000 A /div), CH-3 and CH-4: actual and reference *q*-axis grid currents, respectively (1000 A /div); (c) CH-1: grid voltage (400 V /div), CH-2: grid current (1000 A /div); (d) CH-1: active power supplied to the grid (400 kW /div), CH-2: reactive power transfer between grid-tied converter and the grid (400 kVAR /div).

V. Conclusions

The challenges presented by the intermittent nature of renewable power sources necessitate the development of advanced grid-tied converter technologies to ensure grid stability and reliability. Grid-tied converters play a pivotal role in managing grid synchronization, power quality, reactive power support, and DC link voltage control, especially during adverse grid conditions like voltage dips. The real-time assessment of ride-through capability is a crucial aspect in the design, deployment, and operation of grid-tied converters, aligning with the E.ON Netz grid codes mandating ride-through compliance.

The paper introduced a comprehensive voltage-oriented control strategy meant for grid-tied converters, focusing on achieving unity power factor operation during normal grid condition and demonstrating ride-through capability during symmetrical voltage dip condition. Leveraging the Typhoon HIL604 real-time simulator, extensive testing of grid-tied converter validated the efficacy of the proposed control strategy, highlighting unity power factor operation, and investigating ride-through capability in grid-tied converters within renewable power applications.

Appendix

Coupling inductance	:	$L = 0.6\,\mathrm{mH}$
Coupling resistance	:	$R = 0.1\,\mathrm{m}\Omega$
DC link capacitance	:	$C = 60\,\mathrm{mF}$
DC link voltage	:	$V_{DC} = 1500\,\mathrm{V}$
Grid frequency	:	$f = 50\,\mathrm{Hz}$
Grid voltage (r.m.s.)	:	$V_{LL} = 690\,\mathrm{V}$
Rated converter power	:	$P_{rated} = 1.5\,\mathrm{MW}$

Acknowledgment

The authors express sincere gratitude for the invaluable support extended by the Power & Energy Research Centre (PERC), which provided access to their real-time simulation facility for conducting this research.

References

[1]. Hassan, Q., Viktor, P., Al-Musawi, T.J., Ali, B.M., Algburi, S., Alzoubi, H.M., Al-Jiboory, A.K., Sameen, A.Z., Salman, H.M. and Jaszczur, M., 2024. The renewable energy role in the global energy Transformations. *Renewable Energy Focus*, *48*, p.100545.

[2]. Ang, T.Z., Salem, M., Kamarol, M., Das, H.S., Nazari, M.A. and Prabaharan, N., 2022. A comprehensive study of renewable energy sources: Classifications, challenges and suggestions. *Energy Strategy Reviews*, *43*, p.100939.

[3]. Tripathi, S.M., Tiwari, A.N. and Singh, D., 2015. Grid-integrated permanent magnet synchronous generator based wind energy conversion systems: A technology review. *Renewable and Sustainable Energy Reviews*, *51*, pp.1288-1305.

[4]. Pandey, P., Tripathi, S.M., Goswami, U., Verma, H.K. and Sriwastava, A.K., 2020, October. MIL, SIL, and PIL Simulations of a Grid-Tied Inverter. In *International Conference on Smart Technologies for Energy, Environment, and Sustainable Development* (pp. 657-666). Singapore: Springer Nature Singapore.

[5]. Khalid, M., 2024. Smart grids and renewable energy systems: Perspectives and grid integration challenges. *Energy Strategy Reviews*, *51*, p.101299.

[6]. Tripathi, S.M. and Singh, S., 2020, February. Hardware-in-the-loop simulation of grid-tied converter for unity power factor operation. In *2020 international conference on contemporary computing and applications (IC3A)* (pp. 250-253). IEEE.

[7]. Tripathi, S.M., Singh, U.P., Singh, S., Rai, N.K. and Srivastava, A.K., 2023. Hardware-in-the-loop testing of grid-tied PMSG-based wind power generation system with optimum PI parameters. *e-Prime-Advances in Electrical Engineering, Electronics and Energy*, *5*, p.100282.

[8]. Tripathi, S.M., Tiwari, A.N. and Singh, D., 2016. Optimum design of proportional-integral controllers in grid-integrated PMSG-based wind energy conversion system. *International Transactions on Electrical Energy Systems*, *26*(5), pp.1006-1031.

[9]. Kazmierkowski, M.P. and Malesani, L., 1998. Current control techniques for three-phase voltage-source PWM converters: A survey. *IEEE Transactions on industrial electronics*, *45*(5), pp.691-703.

[10]. Blaabjerg, F., Teodorescu, R., Liserre, M. and Timbus, A.V., 2006. Overview of control and grid synchronization for distributed power generation systems. *IEEE Transactions on industrial electronics*, *53*(5), pp.1398-1409.

[11]. Tripathi, S.M., Tiwari, A.N. and Singh, D., 2019. Low-voltage ride-through enhancement with the ω and T controls of PMSG in a grid-integrated wind generation system. *IET Generation, Transmission & Distribution*, *13*(10), pp.1979-1988.

[12]. Athari, H., Niroomand, M. and Ataei, M., 2017. Review and classification of control systems in grid-tied inverters. *Renewable and Sustainable Energy Reviews*, *72*, pp.1167-1176.

[13]. Liu, Q., Caldognetto, T. and Buso, S., 2019. Review and comparison of grid-tied inverter controllers in microgrids. *IEEE Transactions on Power Electronics*, *35*(7), pp.7624-7639.

[14]. Cao, Y., Zhao, Q., Ye, Y. and Xiong, Y., 2019. ADRC-based current control for grid-tied inverters: Design, analysis, and verification. *IEEE transactions on industrial electronics*, *67*(10), pp.8428-8437.
[15]. Zhao, J., Wu, W., Shuai, Z., Luo, A., Chung, H.S.H. and Blaabjerg, F., 2019. Robust control parameters design of PBC controller for LCL-filtered grid-tied inverter. *IEEE Transactions on Power Electronics*, *35*(8), pp.8102-8115.
[16]. Liu, A., Hou, C., Zhu, M. and Dai, N., 2024. Power Synchronization Control of Grid-Tied Inverter: Phase Error Modeling for Unified System Design. *IEEE Journal of Emerging and Selected Topics in Power Electronics*.
[17]. Elangovan, P. and Mohanty, N.K., 2024. An Adaptive Grid-Tied Inverter Control Scheme for Power Quality Enrichment in Photovoltaic System. *Iranian Journal of Science and Technology, Transactions of Electrical Engineering*, *48*(1), pp.303-315.
[18]. Boscaino, V., Ditta, V., Marsala, G., Panzavecchia, N., Tinè, G., Cosentino, V., Cataliotti, A. and Di Cara, D., 2024. Grid-connected photovoltaic inverters: Grid codes, topologies and control techniques. *Renewable and Sustainable Energy Reviews*, *189*, p.113903.
[19]. Al-Shetwi, A.Q., Sujod, M.Z., Blaabjerg, F. and Yang, Y., 2019. Fault ride-through control of grid-connected photovoltaic power plants: A review. *Solar Energy*, *180*, pp.340-350.
[20]. Mahmoud, M.M., Atia, B.S., Esmail, Y.M., Bajaj, M., Mbadjoun Wapet, D.E., Ratib, M.K., Biplob Hossain, M., AboRas, K.M. and Abdel-Rahim, A.M.M., 2023. Evaluation and comparison of different methods for improving fault ride-through capability in grid-tied permanent magnet synchronous wind generators. *International Transactions on Electrical Energy Systems*, *2023*, pp.1-22.
[21]. Zeb, K., Islam, S.U., Khan, I., Uddin, W., Ishfaq, M., Busarello, T.D.C., Muyeen, S.M., Ahmad, I. and Kim, H.J., 2022. Faults and Fault Ride Through strategies for grid-connected photovoltaic system: A comprehensive review. *Renewable and Sustainable Energy Reviews*, *158*, p.112125.
[22]. Dansoko, M., Nkwawo, H., Floret, F., Goma, R., Diourté, B., Arzande, A. and Vannier, J.C., 2018. Marine turbine system directly connected to electrical grid: Experimental implementations using a nonlinear and robust control. *Ocean Engineering*, *149*, pp.260-267.
[23]. Noman, M., Li, G., Wang, K. and Han, B., 2021. Electrical control strategy for an ocean energy conversion system. *Protection and Control of Modern Power Systems*, *6*(2), pp.1-18.
[24]. IRENA (2022). Grid codes for renewable powered systems. *International renewable energy agency, Abu Dhabi. Available [Online] https://www.irena.org/-/media/Files/IRENA/Agency/Publication/2022/Apr/IRENA_Grid_Codes_Renewable_Systems_2022.pdf?rev=986f108cbe5e47b98d17fca93eee6c86*